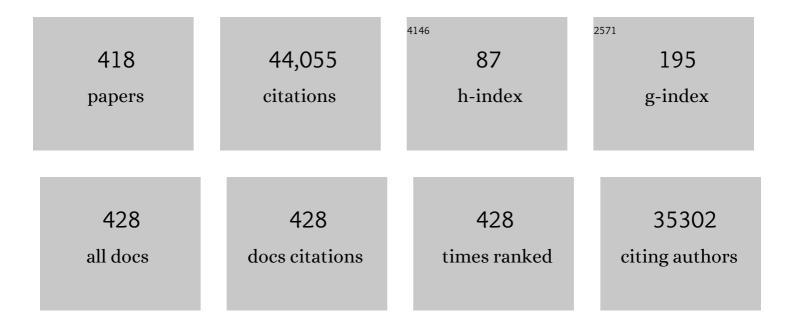
List of Publications by Year in descending order

Source: https://exaly.com/author-pdf/8152480/publications.pdf Version: 2024-02-01



#	Article	IF	CITATIONS
1	How does artificial intelligence in radiology improve efficiency and health outcomes?. Pediatric Radiology, 2022, 52, 2087-2093.	2.0	59
2	Streaming Convolutional Neural Networks for End-to-End Learning With Multi-Megapixel Images. IEEE Transactions on Pattern Analysis and Machine Intelligence, 2022, 44, 1581-1590.	13.9	28
3	Automated COVID-19 Grading With Convolutional Neural Networks in Computed Tomography Scans: A Systematic Comparison. IEEE Transactions on Artificial Intelligence, 2022, 3, 129-138.	4.7	9
4	Scan-based competing death risk model for re-evaluating lung cancer computed tomography screening eligibility. European Respiratory Journal, 2022, 59, 2101613.	6.7	5
5	Imageâ€based automated Psoriasis Area Severity Index scoring by Convolutional Neural Networks. Journal of the European Academy of Dermatology and Venereology, 2022, 36, 68-75.	2.4	17
6	Diffuse idiopathic skeletal hyperostosis is associated with incident stroke in patients with increased cardiovascular risk. Rheumatology, 2022, 61, 2867-2874.	1.9	9
7	Robust Segmentation Models Using an Uncertainty Slice Sampling-Based Annotation Workflow. IEEE Access, 2022, 10, 4728-4738.	4.2	8
8	Automatic Placenta Localization From Ultrasound Imaging in a Resource-Limited Setting Using a Predefined Ultrasound Acquisition Protocol and Deep Learning. Ultrasound in Medicine and Biology, 2022, 48, 663-674.	1.5	6
9	Automated estimation of total lung volume using chest radiographs and deep learning. Medical Physics, 2022, 49, 4466-4477.	3.0	5
10	The Medical Segmentation Decathlon. Nature Communications, 2022, 13, .	12.8	252
11	Prostate158 - An expert-annotated 3T MRI dataset and algorithm for prostate cancer detection. Computers in Biology and Medicine, 2022, 148, 105817.	7.0	17
12	Automated Assessment of COVID-19 Reporting and Data System and Chest CT Severity Scores in Patients Suspected of Having COVID-19 Using Artificial Intelligence. Radiology, 2021, 298, E18-E28.	7.3	116
13	Lung cancer screening by nodule volume in Lung-RADS v1.1: negative baseline CT yields potential for increased screening interval. European Radiology, 2021, 31, 1956-1968.	4.5	24
14	Anisotropic 3D Multi-Stream CNN for Accurate Prostate Segmentation from Multi-Planar MRI. Computer Methods and Programs in Biomedicine, 2021, 200, 105821.	4.7	32
15	The Potential of Artificial Intelligence to Analyze Chest Radiographs for Signs of COVID-19 Pneumonia. Radiology, 2021, 299, E214-E215.	7.3	12
16	Combining pulmonary and cardiac computed tomography biomarkers for disease-specific risk modelling in lung cancer screening. European Respiratory Journal, 2021, 58, 2003386.	6.7	8
17	Computer-aided diagnosis of masses in breast computed tomography imaging: deep learning model with combined handcrafted and convolutional radiomic features. Journal of Medical Imaging, 2021, 8, 024501.	1.5	5
18	Development and Validation of a Convolutional Neural Network for Automated Detection of Scaphoid Fractures on Conventional Radiographs. Radiology: Artificial Intelligence, 2021, 3, e200260.	5.8	20

#	Article	IF	CITATIONS
19	Artificial intelligence in radiology: 100 commercially available products and their scientific evidence. European Radiology, 2021, 31, 3797-3804.	4.5	178
20	Artificial intelligence for detection and characterization of pulmonary nodules in lung cancer CT screening: ready for practice?. Translational Lung Cancer Research, 2021, 10, 2378-2388.	2.8	33
21	A Review of Deep Learning in Medical Imaging: Imaging Traits, Technology Trends, Case Studies With Progress Highlights, and Future Promises. Proceedings of the IEEE, 2021, 109, 820-838.	21.3	339
22	Visceral Adipose Tissue and Different Measures of Adiposity in Different Severities of Diffuse Idiopathic Skeletal Hyperostosis. Journal of Personalized Medicine, 2021, 11, 663.	2.5	14
23	Deep learning with robustness to missing data: A novel approach to the detection of COVID-19. PLoS ONE, 2021, 16, e0255301.	2.5	3
24	Deep learning for chest X-ray analysis: A survey. Medical Image Analysis, 2021, 72, 102125.	11.6	196
25	Deep Learning for Malignancy Risk Estimation of Pulmonary Nodules Detected at Low-Dose Screening CT. Radiology, 2021, 300, 438-447.	7.3	65
26	CNN-based lung CT registration with multiple anatomical constraints. Medical Image Analysis, 2021, 72, 102139.	11.6	39
27	Cost-effectiveness of artificial intelligence aided vessel occlusion detection in acute stroke: an early health technology assessment. Insights Into Imaging, 2021, 12, 133.	3.4	23
28	The Association Between Lung Hyperinflation and Coronary Artery Disease in Smokers. Chest, 2021, 160, 858-871.	0.8	7
29	Assisted versus Manual Interpretation of Low-Dose CT Scans for Lung Cancer Screening: Impact on Lung-RADS Agreement. Radiology Imaging Cancer, 2021, 3, e200160.	1.6	9
30	Adversarial attack vulnerability of medical image analysis systems: Unexplored factors. Medical Image Analysis, 2021, 73, 102141.	11.6	35
31	Deep Learning for Lung Cancer Detection on Screening CT Scans: Results of a Large-Scale Public Competition and an Observer Study with 11 Radiologists. Radiology: Artificial Intelligence, 2021, 3, e210027.	5.8	24
32	Stacked Bidirectional Convolutional LSTMs for Deriving 3D Non-Contrast CT From Spatiotemporal 4D CT. IEEE Transactions on Medical Imaging, 2020, 39, 985-996.	8.9	17
33	Disease Progression Modeling in Chronic Obstructive Pulmonary Disease. American Journal of Respiratory and Critical Care Medicine, 2020, 201, 294-302.	5.6	56
34	Automated deep-learning system for Gleason grading of prostate cancer using biopsies: a diagnostic study. Lancet Oncology, The, 2020, 21, 233-241.	10.7	407
35	Machine Learning Characterization of COPD Subtypes. Chest, 2020, 157, 1147-1157.	0.8	44
36	Evaluation of a deep learning system for the joint automated detection of diabetic retinopathy and ageâ€related macular degeneration. Acta Ophthalmologica, 2020, 98, 368-377.	1.1	68

#	Article	IF	CITATIONS
37	Image-level detection of arterial occlusions in 4D-CTA of acute stroke patients using deep learning. Medical Image Analysis, 2020, 66, 101810.	11.6	15
38	BIAS: Transparent reporting of biomedical image analysis challenges. Medical Image Analysis, 2020, 66, 101796.	11.6	59
39	GANs for medical image analysis. Artificial Intelligence in Medicine, 2020, 109, 101938.	6.5	211
40	Fully Automatic Volume Measurement of the Spleen at CT Using Deep Learning. Radiology: Artificial Intelligence, 2020, 2, e190102.	5.8	21
41	Typical CT Features of Intrapulmonary Lymph Nodes: A Review. Radiology: Cardiothoracic Imaging, 2020, 2, e190159.	2.5	8
42	COVID-19 on Chest Radiographs: A Multireader Evaluation of an Artificial Intelligence System. Radiology, 2020, 296, E166-E172.	7.3	167
43	Iterative Augmentation of Visual Evidence for Weakly-Supervised Lesion Localization in Deep Interpretability Frameworks: Application to Color Fundus Images. IEEE Transactions on Medical Imaging, 2020, 39, 3499-3511.	8.9	22
44	ESR/ERS statement paper on lung cancer screening. European Respiratory Journal, 2020, 55, 1900506.	6.7	57
45	Relational Modeling for Robust and Efficient Pulmonary Lobe Segmentation in CT Scans. IEEE Transactions on Medical Imaging, 2020, 39, 2664-2675.	8.9	81
46	A Deep Learning Model for Segmentation of Geographic Atrophy to Study Its Long-Term Natural History. Ophthalmology, 2020, 127, 1086-1096.	5.2	41
47	Cardiomegaly Detection on Chest Radiographs: Segmentation Versus Classification. IEEE Access, 2020, 8, 94631-94642.	4.2	32
48	Computer-aided diagnosis for World Health Organization-defined chest radiograph primary-endpoint pneumonia in children. Pediatric Radiology, 2020, 50, 482-491.	2.0	48
49	Computer aided detection of tuberculosis on chest radiographs: An evaluation of the CAD4TB v6 system. Scientific Reports, 2020, 10, 5492.	3.3	85
50	CO-RADS: A Categorical CT Assessment Scheme for Patients Suspected of Having COVID-19—Definition and Evaluation. Radiology, 2020, 296, E97-E104.	7.3	693
51	ESR/ERS statement paper on lung cancer screening. European Radiology, 2020, 30, 3277-3294.	4.5	83
52	Evaluation of computer aided detection of tuberculosis on chest radiography among people with diabetes in Karachi Pakistan. Scientific Reports, 2020, 10, 6276.	3.3	10
53	Immunoglobulin E as a Biomarker for the Overlap of Atopic Asthma and Chronic Obstructive Pulmonary Disease. Chronic Obstructive Pulmonary Diseases (Miami, Fla ), 2020, 7, 1-12.	0.7	18
54	Feasibility of end-to-end trainable two-stage U-Net for detection of axillary lymph nodes in		2

contrast-enhanced CT based on sparse annotations. , 2020, , .

#	Article	IF	CITATIONS
55	Observer variability for Lung-RADS categorisation of lung cancer screening CTs: impact on patient management. European Radiology, 2019, 29, 924-931.	4.5	46
56	iW-Net: an automatic and minimalistic interactive lung nodule segmentation deep network. Scientific Reports, 2019, 9, 11591.	3.3	52
57	Image Level Training and Prediction: Intracranial Hemorrhage Identification in 3D Non-Contrast CT. IEEE Access, 2019, 7, 92355-92364.	4.2	48
58	Automated chest X-ray reading for tuberculosis in the Philippines to improve case detection: a cohort study. International Journal of Tuberculosis and Lung Disease, 2019, 23, 805-810.	1.2	10
59	Epithelium segmentation using deep learning in H&E-stained prostate specimens with immunohistochemistry as reference standard. Scientific Reports, 2019, 9, 864.	3.3	107
60	Sex Differences in Coronary Artery and Thoracic Aorta Calcification and Their Association With Cardiovascular Mortality in Heavy Smokers. JACC: Cardiovascular Imaging, 2019, 12, 1808-1817.	5.3	25
61	Google's lung cancer AI: a promising tool that needs further validation. Nature Reviews Clinical Oncology, 2019, 16, 532-533.	27.6	26
62	Reducing inter-observer variability and interaction time of MR liver volumetry by combining automatic CNN-based liver segmentation and manual corrections. PLoS ONE, 2019, 14, e0217228.	2.5	40
63	The St. George's Respiratory Questionnaire Definition of Chronic Bronchitis May Be aÂBetter Predictor of COPD Exacerbations Compared With the Classic Definition. Chest, 2019, 156, 685-695.	0.8	40
64	Multiclass Brain Tissue Segmentation in 4D CT Using Convolutional Neural Networks. IEEE Access, 2019, 7, 51557-51569.	4.2	12
65	Predicting all-cause and lung cancer mortality using emphysema score progression rate between baseline and follow-up chest CT images: A comparison of risk model performances. PLoS ONE, 2019, 14, e0212756.	2.5	4
66	Genetic landscape of chronic obstructive pulmonary disease identifies heterogeneous cell-type and phenotype associations. Nature Genetics, 2019, 51, 494-505.	21.4	257
67	Iterative fully convolutional neural networks for automatic vertebra segmentation and identification. Medical Image Analysis, 2019, 53, 142-155.	11.6	170
68	Intracerebral Haemorrhage Segmentation in Non-Contrast CT. Scientific Reports, 2019, 9, 17858.	3.3	33
69	From Detection of Individual Metastases to Classification of Lymph Node Status at the Patient Level: The CAMELYON17 Challenge. IEEE Transactions on Medical Imaging, 2019, 38, 550-560.	8.9	269
70	Automated Fetal Head Detection and Circumference Estimation from Free-Hand Ultrasound Sweeps Using Deep Learning in Resource-Limited Countries. Ultrasound in Medicine and Biology, 2019, 45, 773-785.	1.5	59
71	Predicting Malignancy Risk of Screen-Detected Lung Nodules–Mean Diameter or Volume. Journal of Thoracic Oncology, 2019, 14, 203-211.	1.1	34
72	Deep Learning for Triage of Chest Radiographs: Should Every Institution Train Its Own System?. Radiology, 2019, 290, 545-546.	7.3	8

#	Article	IF	CITATIONS
73	Airway wall thickening on CT: Relation to smoking status and severity of COPD. Respiratory Medicine, 2019, 146, 36-41.	2.9	47
74	Integrative Genomics Analysis Identifies ACVR1B as a Candidate Causal Gene of Emphysema Distribution. American Journal of Respiratory Cell and Molecular Biology, 2019, 60, 388-398.	2.9	15
75	mlVIRNET: Multilevel Variational Image Registration Network. Lecture Notes in Computer Science, 2019, , 257-265.	1.3	32
76	Handling label noise through model confidence and uncertainty: application to chest radiograph classification. , 2019, , .		9
77	Resolution-agnostic tissue segmentation in whole-slide histopathology images with convolutional neural networks. PeerJ, 2019, 7, e8242.	2.0	39
78	In vivo growth of 60 non-screening detected lung cancers: a computed tomography study. European Respiratory Journal, 2018, 51, 1702183.	6.7	12
79	Automatic Calcium Scoring in Low-Dose Chest CT Using Deep Neural Networks With Dilated Convolutions. IEEE Transactions on Medical Imaging, 2018, 37, 615-625.	8.9	176
80	Asthma Is a Risk Factor for Respiratory Exacerbations Without Increased Rate of Lung Function Decline. Chest, 2018, 153, 368-377.	0.8	14
81	Automatic segmentation of the solid core and enclosed vessels in subsolid pulmonary nodules. Scientific Reports, 2018, 8, 646.	3.3	14
82	Lung cancer risk to personalise annual and biennial follow-up computed tomography screening. Thorax, 2018, 73, 626-633.	5.6	33
83	Detection of Subsolid Nodules in Lung Cancer Screening. Investigative Radiology, 2018, 53, 441-449.	6.2	35
84	Efficient organ localization using multi-label convolutional neural networks in thorax-abdomen CT scans. Physics in Medicine and Biology, 2018, 63, 085003.	3.0	29
85	Incidental perifissural nodules on routine chest computed tomography: lung cancer or not?. European Radiology, 2018, 28, 1095-1101.	4.5	28
86	Lobar Emphysema Distribution Is Associated With 5-Year Radiological Disease Progression. Chest, 2018, 153, 65-76.	0.8	36
87	ES01.03 Deep Machine Learning for Screening LDCT. Journal of Thoracic Oncology, 2018, 13, S190.	1.1	0
88	Why rankings of biomedical image analysis competitions should be interpreted with care. Nature Communications, 2018, 9, 5217.	12.8	198
89	Towards an Automatic Lung Cancer Screening System in Low Dose Computed Tomography. Lecture Notes in Computer Science, 2018, , 310-318.	1.3	8
90	MA20.09 Improved Lung Cancer and Mortality Prediction Accuracy Using Survival Models Based on Semi-Automatic CT Image Measurements. Journal of Thoracic Oncology, 2018, 13, S428.	1.1	0

#	Article	IF	CITATIONS
91	Automatic liver tumor segmentation in CT with fully convolutional neural networks and object-based postprocessing. Scientific Reports, 2018, 8, 15497.	3.3	155
92	Long-Term Active Surveillance of Screening Detected Subsolid Nodules is a Safe Strategy to Reduce Overtreatment. Journal of Thoracic Oncology, 2018, 13, 1454-1463.	1.1	51
93	Brock malignancy risk calculator for pulmonary nodules: validation outside a lung cancer screening population. Thorax, 2018, 73, 857-863.	5.6	36
94	Classification of CT Pulmonary Opacities as Perifissural Nodules: Reader Variability. Radiology, 2018, 288, 867-875.	7.3	40
95	Accuracy of an automated system for tuberculosis detection on chest radiographs in high-risk screening. International Journal of Tuberculosis and Lung Disease, 2018, 22, 567-571.	1.2	24
96	Deep learning approach for the detection and quantification of intraretinal cystoid fluid in multivendor optical coherence tomography. Biomedical Optics Express, 2018, 9, 1545.	2.9	124
97	Comparison Study of Low-Cost Ultrasound Devices for Estimation of Gestational Age in Resource-Limited Countries. Ultrasound in Medicine and Biology, 2018, 44, 2250-2260.	1.5	7
98	Small airway segmentation in thoracic computed tomography scans: a machine learning approach. Physics in Medicine and Biology, 2018, 63, 155024.	3.0	12
99	Automated measurement of fetal head circumference using 2D ultrasound images. PLoS ONE, 2018, 13, e0200412.	2.5	117
100	Computer-assisted chest radiography reading for tuberculosis screening in people living with diabetes mellitus. International Journal of Tuberculosis and Lung Disease, 2018, 22, 1088-1094.	1.2	24
101	Evaluation of the diagnostic accuracy of Computer-Aided Detection of tuberculosis on Chest radiography among private sector patients in Pakistan. Scientific Reports, 2018, 8, 12339.	3.3	45
102	Visual discrimination of screen-detected persistent from transient subsolid nodules: An observer study. PLoS ONE, 2018, 13, e0191874.	2.5	8
103	Using deep convolutional neural networks to identify and classify tumor-associated stroma in diagnostic breast biopsies. Modern Pathology, 2018, 31, 1502-1512.	5.5	145
104	Iterative convolutional neural networks for automatic vertebra identification and segmentation in CT images. , 2018, , .		5
105	Student beats the teacher: deep neural networks for lateral ventricles segmentation in brain MR. , 2018, , .		3
106	Real-Life Artificial Intelligence Applications. Journal of the Belgian Society of Radiology, 2018, 102, .	0.3	1
107	Image Analysis for Moving Organ, Breast, and Thoracic Images. Lecture Notes in Computer Science, 2018, , .	1.3	3
108	Subsolid pulmonary nodule morphology and associated patient characteristics in a routine clinical population. European Radiology, 2017, 27, 689-696.	4.5	16

#	Article	IF	CITATIONS
109	Discriminating solitary cysts from soft tissue lesions in mammography using a pretrained deep convolutional neural network. Medical Physics, 2017, 44, 1017-1027.	3.0	84
110	Comparison of the effects of model-based iterative reconstruction and filtered back projection algorithms on software measurements in pulmonary subsolid nodules. European Radiology, 2017, 27, 3266-3274.	4.5	17
111	Fast and effective quantification of symmetry in medical images for pathology detection: Application to chest radiography. Medical Physics, 2017, 44, 2242-2256.	3.0	7
112	Fifty years of computer analysis in chest imaging: rule-based, machine learning, deep learning. Radiological Physics and Technology, 2017, 10, 23-32.	1.9	133
113	Deep multi-scale location-aware 3D convolutional neural networks for automated detection of lacunes of presumed vascular origin. NeuroImage: Clinical, 2017, 14, 391-399.	2.7	99
114	Organ detection in thorax abdomen CT using multi-label convolutional neural networks. , 2017, , .		4
115	Automatic cerebrospinal fluid segmentation in non-contrast CT images using a 3D convolutional network. , 2017, , .		3
116	Fovea detection in optical coherence tomography using convolutional neural networks. Proceedings of SPIE, 2017, , .	0.8	0
117	Computed tomography quantification of tracheal abnormalities in COPD and their influence on airflow limitation. Medical Physics, 2017, 44, 3594-3603.	3.0	5
118	Computed tomographic findings in subjects who died from respiratory disease in the National Lung Screening Trial. European Respiratory Journal, 2017, 49, 1601814.	6.7	26
119	Towards automatic pulmonary nodule management in lung cancer screening with deep learning. Scientific Reports, 2017, 7, 46479.	3.3	230
120	Malignancy estimation of Lung-RADS criteria for subsolid nodules on CT: accuracy of low and high risk spectrum when using NLST nodules. European Radiology, 2017, 27, 4672-4679.	4.5	15
121	Fast interactive segmentation of the pulmonary lobes from thoracic computed tomography data. Physics in Medicine and Biology, 2017, 62, 6649-6665.	3.0	11
122	Lung-RADS Category 4X: Does It Improve Prediction of Malignancy in Subsolid Nodules?. Radiology, 2017, 284, 264-271.	7.3	46
123	White Matter and Gray Matter Segmentation in 4D Computed Tomography. Scientific Reports, 2017, 7, 119.	3.3	21
124	Malignancy risk estimation of screen-detected nodules at baseline CT: comparison of the PanCan model, Lung-RADS and NCCN guidelines. European Radiology, 2017, 27, 4019-4029.	4.5	42
125	Robust cranial cavity segmentation in CT and CT perfusion images of trauma and suspected stroke patients. Medical Image Analysis, 2017, 36, 216-228.	11.6	20
126	Use of Volumetry for Lung Nodule Management: Theory and Practice. Radiology, 2017, 284, 630-644.	7.3	111

#	Article	IF	CITATIONS
127	A survey on deep learning in medical image analysis. Medical Image Analysis, 2017, 42, 60-88.	11.6	7,976
128	Diagnostic Assessment of Deep Learning Algorithms for Detection of Lymph Node Metastases in Women With Breast Cancer. JAMA - Journal of the American Medical Association, 2017, 318, 2199.	7.4	2,003
129	Robust Segmentation of the Full Cerebral Vasculature in 4D CT of Suspected Stroke Patients. Scientific Reports, 2017, 7, 15622.	3.3	38
130	Comparison of different methods for tissue segmentation in histopathological whole-slide images. , 2017, , .		29
131	Validation, comparison, and combination of algorithms for automatic detection of pulmonary nodules in computed tomography images: The LUNA16 challenge. Medical Image Analysis, 2017, 42, 1-13.	11.6	710
132	Location Sensitive Deep Convolutional Neural Networks for Segmentation of White Matter Hyperintensities. Scientific Reports, 2017, 7, 5110.	3.3	171
133	The importance of stain normalization in colorectal tissue classification with convolutional networks. , 2017, , .		105
134	Improving airway segmentation in computed tomography using leak detection with convolutional networks. Medical Image Analysis, 2017, 36, 52-60.	11.6	78
135	Large scale deep learning for computer aided detection of mammographic lesions. Medical Image Analysis, 2017, 35, 303-312.	11.6	728
136	Interleaving cerebral CT perfusion with neck CT angiography part I. Proof of concept and accuracy of cerebral perfusion values. European Radiology, 2017, 27, 2649-2656.	4.5	9
137	Interleaving cerebral CT perfusion with neck CT angiography. Part II: clinical implementation and image quality. European Radiology, 2017, 27, 2411-2418.	4.5	12
138	MA 14.11 Malignancy Risk Prediction of Pulmonary Nodule in Lung Cancer Screening – Diameter Or Volumetric Measurement. Journal of Thoracic Oncology, 2017, 12, S1859-S1860.	1.1	0
139	Automated Staging of Age-Related Macular Degeneration Using Optical Coherence Tomography. , 2017, 58, 2318.		93
140	Automatic detection of the foveal center in optical coherence tomography. Biomedical Optics Express, 2017, 8, 5160.	2.9	26
141	Robust total retina thickness segmentation in optical coherence tomography images using convolutional neural networks. Biomedical Optics Express, 2017, 8, 3292.	2.9	106
142	Automatic versus human reading of chest X-rays in the Zambia National Tuberculosis Prevalence Survey. International Journal of Tuberculosis and Lung Disease, 2017, 21, 880-886.	1.2	25
143	Malignancy risk estimation of pulmonary nodules in screening CTs: Comparison between a computer model and human observers. PLoS ONE, 2017, 12, e0185032.	2.5	28
144	Normalized emphysema scores on low dose CT: Validation as an imaging biomarker for mortality. PLoS ONE, 2017, 12, e0188902.	2.5	14

#	Article	IF	CITATIONS
145	Transfer Learning for Domain Adaptation in MRI: Application in Brain Lesion Segmentation. Lecture Notes in Computer Science, 2017, , 516-524.	1.3	167
146	Context-aware stacked convolutional neural networks for classification of breast carcinomas in whole-slide histopathology images. Journal of Medical Imaging, 2017, 4, 1.	1.5	126
147	A step towards measuring the fetal head circumference with the use of obstetric ultrasound in a low resource setting. Proceedings of SPIE, 2017, , .	0.8	3
148	Combining Automated Image Analysis with Obstetric Sweeps for Prenatal Ultrasound Imaging in Developing Countries. Lecture Notes in Computer Science, 2017, , 105-112.	1.3	2
149	Smokers with emphysema and small airway disease on computed tomography have lower bone density. International Journal of COPD, 2016, 11, 1207.	2.3	15
150	Optimization Strategies for Interactive Classification of Interstitial Lung Disease Textures. Frontiers in ICT, 2016, 3, .	3.6	0
151	The Effect of Supplementary Bone-Suppressed Chest Radiographs on the Assessment of a Variety of Common Pulmonary Abnormalities. Journal of Thoracic Imaging, 2016, 31, 119-125.	1.5	7
152	Automatic differentiation of color fundus images containing drusen or exudates using a contextual spatial pyramid approach. Biomedical Optics Express, 2016, 7, 709.	2.9	8
153	An automated tuberculosis screening strategy combining X-ray-based computer-aided detection and clinical information. Scientific Reports, 2016, 6, 25265.	3.3	100
154	Deep learning as a tool for increased accuracy and efficiency of histopathological diagnosis. Scientific Reports, 2016, 6, 26286.	3.3	764
155	Semi-automatic classification of textures in thoracic CT scans. Physics in Medicine and Biology, 2016, 61, 5906-5924.	3.0	6
156	Fleischner recommendations for the management of subsolid pulmonary nodules: high awareness but limited conformance – a survey study. European Radiology, 2016, 26, 3840-3849.	4.5	28
157	Software performance in segmenting ground-glass and solid components of subsolid nodules in pulmonary adenocarcinomas. European Radiology, 2016, 26, 4465-4474.	4.5	42
158	Follow-up of CT-derived airway wall thickness: Correcting for changes in inspiration level improves reliability. European Journal of Radiology, 2016, 85, 2008-2013.	2.6	8
159	Deep convolutional neural networks for automatic coronary calcium scoring in a screening study with low-dose chest CT. Proceedings of SPIE, 2016, , .	0.8	22
160	Non-uniform patch sampling with deep convolutional neural networks for white matter hyperintensity segmentation. , 2016, , .		41
161	The effect of late-phase contrast enhancement on semi-automatic software measurements of CT attenuation and volume of part-solid nodules in lung adenocarcinomas. European Journal of Radiology, 2016, 85, 1174-1180.	2.6	15
162	Guest Editorial Deep Learning in Medical Imaging: Overview and Future Promise of an Exciting New Technique. IEEE Transactions on Medical Imaging, 2016, 35, 1153-1159.	8.9	1,261

#	Article	IF	CITATIONS
163	Content-Based Image Retrieval by Metric Learning From Radiology Reports: Application to Interstitial Lung Diseases. IEEE Journal of Biomedical and Health Informatics, 2016, 20, 281-292.	6.3	33
164	Pulmonary Nodule Detection in CT Images: False Positive Reduction Using Multi-View Convolutional Networks. IEEE Transactions on Medical Imaging, 2016, 35, 1160-1169.	8.9	926
165	Computer Vision Tool and Technician as First Reader of Lung Cancer Screening CT Scans. Journal of Thoracic Oncology, 2016, 11, 709-717.	1.1	30
166	Computer-aided detection of pulmonary nodules: a comparative study using the public LIDC/IDRI database. European Radiology, 2016, 26, 2139-2147.	4.5	87
167	Fast Convolutional Neural Network Training Using Selective Data Sampling: Application to Hemorrhage Detection in Color Fundus Images. IEEE Transactions on Medical Imaging, 2016, 35, 1273-1284.	8.9	335
168	Automatic detection of pleural effusion in chest radiographs. Medical Image Analysis, 2016, 28, 22-32.	11.6	31
169	On Combining Multiple-Instance Learning and Active Learning for Computer-Aided Detection of Tuberculosis. IEEE Transactions on Medical Imaging, 2016, 35, 1013-1024.	8.9	45
170	Normalizing computed tomography data reconstructed with different filter kernels: effect on emphysema quantification. European Radiology, 2016, 26, 478-486.	4.5	52
171	Quantitative Dose Dependency Analysis of Whole-Brain CT Perfusion Imaging. Radiology, 2016, 278, 190-197.	7.3	22
172	A 4D CT digital phantom of an individual human brain for perfusion analysis. PeerJ, 2016, 4, e2683.	2.0	3
173	Screening for pulmonary tuberculosis in a Tanzanian prison and computer-aided interpretation of chest X-rays. Public Health Action, 2015, 5, 249-254.	1.2	19
174	Automatic detection of large pulmonary solid nodules in thoracic CT images. Medical Physics, 2015, 42, 5642-5653.	3.0	109
175	Automated chest-radiography as a triage for Xpert testing in resource-constrained settings: a prospective study of diagnostic accuracy and costs. Scientific Reports, 2015, 5, 12215.	3.3	54
176	Observer Variability for Classification of Pulmonary Nodules on Low-Dose CT Images and Its Effect on Nodule Management. Radiology, 2015, 277, 863-871.	7.3	145
177	Parametric Response Mapping Adds Value to Current Computed Tomography Biomarkers in Diagnosing Chronic Obstructive Pulmonary Disease. American Journal of Respiratory and Critical Care Medicine, 2015, 191, 1084-1086.	5.6	28
178	Automatic Detection of Tuberculosis in Chest Radiographs Using a Combination of Textural, Focal, and Shape Abnormality Analysis. IEEE Transactions on Medical Imaging, 2015, 34, 2429-2442.	8.9	62
179	Automatic detection of spiculation of pulmonary nodules in computed tomography images. , 2015, , .		2
180	Computer-aided detection of lung cancer: combining pulmonary nodule detection systems with a tumor risk prediction model. Proceedings of SPIE, 2015, , .	0.8	2

#	Article	IF	CITATIONS
181	Robust semi-automatic segmentation of pulmonary subsolid nodules in chest computed tomography scans. Physics in Medicine and Biology, 2015, 60, 1307-1323.	3.0	61
182	Airway wall thickness associated with forced expiratory volume in 1 second decline and development of airflow limitation. European Respiratory Journal, 2015, 45, 644-651.	6.7	50
183	Novel Genes for Airway Wall Thickness Identified with Combined Genome-Wide Association and Expression Analyses. American Journal of Respiratory and Critical Care Medicine, 2015, 191, 547-556.	5.6	32
184	Automatic Identification of Reticular Pseudodrusen Using Multimodal Retinal Image Analysis. Investigative Ophthalmology and Visual Science, 2015, 56, 633-639.	3.3	32
185	Interscan variation of semi-automated volumetry of subsolid pulmonary nodules. European Radiology, 2015, 25, 1040-1047.	4.5	24
186	Pulmonary function and CT biomarkers as risk factors for cardiovascular events in male lung cancer screening participants: the NELSON study. European Radiology, 2015, 25, 65-71.	4.5	9
187	Detection and quantification of the solid component in pulmonary subsolid nodules by semiautomatic segmentation. European Radiology, 2015, 25, 488-496.	4.5	58
188	Reduced Bone Density and Vertebral Fractures in Smokers. Men and COPD Patients at Increased Risk. Annals of the American Thoracic Society, 2015, 12, 648-656.	3.2	92
189	Localized Energy-Based Normalization of Medical Images: Application to Chest Radiography. IEEE Transactions on Medical Imaging, 2015, 34, 1965-1975.	8.9	34
190	Predictive Accuracy of the PanCan Lung Cancer Risk Prediction Model -External Validation based on CT from the Danish Lung Cancer Screening Trial. European Radiology, 2015, 25, 3093-3099.	4.5	70
191	Solid, Part-Solid, or Non-Solid?. Investigative Radiology, 2015, 50, 168-173.	6.2	42
192	Automated age-related macular degeneration classification in OCT using unsupervised feature learning. Proceedings of SPIE, 2015, , .	0.8	30
193	Timing-Invariant CT Angiography Derived from CT Perfusion Imaging in Acute Stroke: A Diagnostic Performance Study. American Journal of Neuroradiology, 2015, 36, 1834-1838.	2.4	22
194	Off-the-shelf convolutional neural network features for pulmonary nodule detection in computed tomography scans. , 2015, , .		150
195	Automatic classification of pulmonary peri-fissural nodules in computed tomography using an ensemble of 2D views and a convolutional neural network out-of-the-box. Medical Image Analysis, 2015, 26, 195-202.	11.6	236
196	Bag-of-Frequencies: A Descriptor of Pulmonary Nodules in Computed Tomography Images. IEEE Transactions on Medical Imaging, 2015, 34, 962-973.	8.9	45
197	Towards a close computed tomography monitoring approach for screen detected subsolid pulmonary nodules?. European Respiratory Journal, 2015, 45, 765-773.	6.7	98
198	A Novel Multiple-Instance Learning-Based Approach to Computer-Aided Detection of Tuberculosis on Chest X-Rays. IEEE Transactions on Medical Imaging, 2015, 34, 179-192.	8.9	92

#	Article	IF	CITATIONS
199	Using the Fourth Dimension to Distinguish Between Structures for Anisotropic Diffusion Filtering in 4D CT Perfusion Scans. Lecture Notes in Computer Science, 2015, , 79-87.	1.3	1
200	Bone density is associated with emphysema and air trapping on CT in smokers. , 2015, , .		0
201	Reproducibility of airway wall thickness measurements on CT in a lung cancer screening setting. , 2015, , .		0
202	The Sensitivity and Specificity of Using a Computer Aided Diagnosis Program for Automatically Scoring Chest X-Rays of Presumptive TB Patients Compared with Xpert MTB/RIF in Lusaka Zambia. PLoS ONE, 2014, 9, e93757.	2.5	76
203	Effect of image variation on computer-aided detection systems. Proceedings of SPIE, 2014, , .	0.8	Ο
204	Influence of study design in receiver operating characteristics studies: sequential versus independent reading. Journal of Medical Imaging, 2014, 1, 015501.	1.5	5
205	Interactive lung segmentation in abnormal human and animal chest CT scans. Medical Physics, 2014, 41, 081915.	3.0	7
206	A 4D digital phantom for patient-specific simulation of brain CT perfusion protocols. Medical Physics, 2014, 41, 071907.	3.0	4
207	Computer-aided Detection Improves Detection of Pulmonary Nodules in Chest Radiographs beyond the Support by Bone-suppressed Images. Radiology, 2014, 272, 252-261.	7.3	63
208	Cavity contour segmentation in chest radiographs using supervised learning and dynamic programming. Medical Physics, 2014, 41, 071912.	3.0	5
209	Improving mass candidate detection in mammograms via feature maxima propagation and local feature selection. Medical Physics, 2014, 41, 081904.	3.0	3
210	Multiple-instance learning for computer-aided detection of tuberculosis. Proceedings of SPIE, 2014, , .	0.8	3
211	Chest Radiography: New Technological Developments and Their Applications. Seminars in Respiratory and Critical Care Medicine, 2014, 35, 003-016.	2.1	15
212	Automated detection and quantification of micronodules in thoracic CT scans to identify subjects at risk for silicosis. , 2014, , .		0
213	DIRBoost–An algorithm for boosting deformable image registration: Application to lung CT intra-subject registration. Medical Image Analysis, 2014, 18, 449-459.	11.6	23
214	Automatic detection of subsolid pulmonary nodules in thoracic computed tomography images. Medical Image Analysis, 2014, 18, 374-384.	11.6	214
215	Evaluation of prostate segmentation algorithms for MRI: The PROMISE12 challenge. Medical Image Analysis, 2014, 18, 359-373.	11.6	469
216	Discriminating dominant computed tomography phenotypes in smokers without or with mild COPD. Respiratory Medicine, 2014, 108, 136-143.	2.9	26

#	Article	IF	CITATIONS
217	Comparing algorithms for automated vessel segmentation in computed tomography scans of the lung: the VESSEL12 study. Medical Image Analysis, 2014, 18, 1217-1232.	11.6	131
218	New methods for using computer-aided detection information for the detection of lung nodules on chest radiographs. British Journal of Radiology, 2014, 87, 20140015.	2.2	8
219	Contribution of CT Quantified Emphysema, Air Trapping and Airway Wall Thickness on Pulmonary Function in Male Smokers With and Without COPD. COPD: Journal of Chronic Obstructive Pulmonary Disease, 2014, 11, 503-509.	1.6	39
220	Diagnostic Accuracy of Computer-Aided Detection of Pulmonary Tuberculosis in Chest Radiographs: A Validation Study from Sub-Saharan Africa. PLoS ONE, 2014, 9, e106381.	2.5	77
221	Bone Suppression Increases the Visibility of Invasive Pulmonary Aspergillosis in Chest Radiographs. PLoS ONE, 2014, 9, e108551.	2.5	12
222	Diagnosis of chronic obstructive pulmonary disease in lung cancer screening Computed Tomography scans: independent contribution of emphysema, air trapping and bronchial wall thickening. Respiratory Research, 2013, 14, 59.	3.6	63
223	Rate of progression of CT-quantified emphysema in male current and ex-smokers: a follow-up study. Respiratory Research, 2013, 14, 55.	3.6	31
224	Low-dose CT measurements of airway dimensions and emphysema associated with airflow limitation in heavy smokers: a cross sectional study. Respiratory Research, 2013, 14, 11.	3.6	32
225	Bone suppressed images improve radiologists' detection performance for pulmonary nodules in chest radiographs. European Journal of Radiology, 2013, 82, 2399-2405.	2.6	26
226	Suppression of Translucent Elongated Structures: Applications in Chest Radiography. IEEE Transactions on Medical Imaging, 2013, 32, 2099-2113.	8.9	25
227	Automatic Segmentation of the Pulmonary Lobes From Chest CT Scans Based on Fissures, Vessels, and Bronchi. IEEE Transactions on Medical Imaging, 2013, 32, 210-222.	8.9	84
228	Improved texture analysis for automatic detection of tuberculosis (TB) on chest radiographs with bone suppression images. , 2013, , .		11
229	Automated segmentation of pulmonary structures in thoracic computed tomography scans: a review. Physics in Medicine and Biology, 2013, 58, R187-R220.	3.0	110
230	A pattern recognition framework for vessel segmentation in 4D CT of the brain. , 2013, , .		1
231	Normalization of CT scans reconstructed with different kernels to reduce variability in emphysema measurements. , 2013, , .		1
232	Automatic age-related macular degeneration detection and staging. Proceedings of SPIE, 2013, , .	0.8	1
233	Normalization of chest radiographs. , 2013, , .		4
234	Timing-Invariant Imaging of Collateral Vessels in Acute Ischemic Stroke. Stroke, 2013, 44, 2194-2199.	2.0	93

#	Article	IF	CITATIONS
235	Computer-Aided Segmentation and Volumetry of Artificial Ground-Glass Nodules at Chest CT. American Journal of Roentgenology, 2013, 201, 295-300.	2.2	29
236	Automated localization of costophrenic recesses and costophrenic angle measurement on frontal chest radiographs. Proceedings of SPIE, 2013, , .	0.8	7
237	A Bag of Words approach for discriminating between retinal images containing exudates or drusen. , 2013, , .		11
238	Subphenotypes of Mild-to-Moderate COPD by Factor and Cluster Analysis of Pulmonary Function, CT Imaging and Breathomics in a Population-Based Survey. COPD: Journal of Chronic Obstructive Pulmonary Disease, 2013, 10, 277-285.	1.6	43
239	Foreign object detection and removal to improve automated analysis of chest radiographs. Medical Physics, 2013, 40, 071901.	3.0	6
240	Detection of tuberculosis using digital chest radiography: automated reading vs. interpretation by clinical officers. International Journal of Tuberculosis and Lung Disease, 2013, 17, 1613-1620.	1.2	71
241	Impact of bone suppression imaging on the detection of lung nodules in chest radiographs: analysis of multiple reading sessions. Proceedings of SPIE, 2013, , .	0.8	1
242	A hardware implementation of a levelset algorithm for carotid lumen segmentation in CTA. Proceedings of SPIE, 2013, , .	0.8	0
243	Automatic Drusen Quantification and Risk Assessment of Age-Related Macular Degeneration on Color Fundus Images. , 2013, 54, 3019.		40
244	Non-solid lung nodules on low-dose computed tomography: comparison of detection rate between 3 visualization techniques. Cancer Imaging, 2013, 13, 150-154.	2.8	4
245	CT Air Trapping Is Independently Associated with Lung Function Reduction over Time. PLoS ONE, 2013, 8, e61783.	2.5	11
246	Computed Tomography Structural Lung Changes in Discordant Airflow Limitation. PLoS ONE, 2013, 8, e65177.	2.5	14
247	Semi-Automatic Quantification of Subsolid Pulmonary Nodules: Comparison with Manual Measurements. PLoS ONE, 2013, 8, e80249.	2.5	25
248	Improved Arterial Visualization in Cerebral CT Perfusion–Derived Arteriograms Compared with Standard CT Angiography: A Visual Assessment Study. American Journal of Neuroradiology, 2012, 33, 2171-2177.	2.4	8
249	Automatic classication of pulmonary function in COPD patients using trachea analysis in chest CT scans. Proceedings of SPIE, 2012, , .	0.8	2
250	Timing-Invariant Reconstruction for Deriving High-Quality CT Angiographic Data from Cerebral CT Perfusion Data. Radiology, 2012, 263, 216-225.	7.3	64
251	Computed tomography-quantified emphysema distribution is associated with lung function decline. European Respiratory Journal, 2012, 40, 844-850.	6.7	70
252	Normal Range of Emphysema and Air Trapping on CT in Young Men. American Journal of Roentgenology, 2012, 199, 336-340.	2.2	51

#	Article	IF	CITATIONS
253	Pulmonary Perifissural Nodules on CT Scans: Rapid Growth Is Not a Predictor of Malignancy. Radiology, 2012, 265, 611-616.	7.3	153
254	DIRBoost: An algorithm for boosting deformable image registration. , 2012, , .		3
255	Coronary Artery Calcium Can Predict All-Cause Mortality and Cardiovascular Events on Low-Dose CT Screening for Lung Cancer. American Journal of Roentgenology, 2012, 198, 505-511.	2.2	146
256	Toward automatic regional analysis of pulmonary function using inspiration and expiration thoracic CT. Medical Physics, 2012, 39, 1650-1662.	3.0	43
257	Lung Function Decline in Male Heavy Smokers Relates to Baseline Airflow Obstruction Severity. Chest, 2012, 142, 1530-1538.	0.8	25
258	Brain tissue segmentation in 4D CT using voxel classification. Proceedings of SPIE, 2012, , .	0.8	2
259	Automatic Coronary Calcium Scoring in Low-Dose Chest Computed Tomography. IEEE Transactions on Medical Imaging, 2012, 31, 2322-2334.	8.9	112
260	Early Identification of Small Airways Disease on Lung Cancer Screening CT: Comparison of Current Air Trapping Measures. Lung, 2012, 190, 629-633.	3.3	56
261	Potential of a Standalone Computer-Aided Detection System for Breast Cancer Detection in Screening Mammography. Lecture Notes in Computer Science, 2012, , 682-689.	1.3	0
262	Clavicle segmentation in chest radiographs. Medical Image Analysis, 2012, 16, 1490-1502.	11.6	40
263	Supervised quality assessment of medical image registration: Application to intra-patient CT lung registration. Medical Image Analysis, 2012, 16, 1521-1531.	11.6	42
264	Extraction of Airways From CT (EXACT'09). IEEE Transactions on Medical Imaging, 2012, 31, 2093-2107.	8.9	173
265	On Combining Algorithms for Deformable Image Registration. Lecture Notes in Computer Science, 2012, , 256-265.	1.3	5
266	The relationship between lung function impairment and quantitative computed tomography in chronic obstructive pulmonary disease. European Radiology, 2012, 22, 120-128.	4.5	56
267	A method for the automatic quantification of the completeness of pulmonary fissures: evaluation in a database of subjects with severe emphysema. European Radiology, 2012, 22, 302-309.	4.5	50
268	Quantitative Computed Tomography in COPD: Possibilities and Limitations. Lung, 2012, 190, 133-145.	3.3	107
269	Contextual computer-aided detection: Improving bright lesion detection in retinal images and coronary calcification identification in CT scans. Medical Image Analysis, 2012, 16, 50-62.	11.6	41
270	Cluster Analysis Identifies COPD Subphenotypes By Combining Pulmonary Function, CT Imaging And Breathomics. , 2011, , .		0

#	Article	IF	CITATIONS
271	Computer-aided detection as a decision assistant in chest radiography. , 2011, , .		3
272	On Combining Computer-Aided Detection Systems. IEEE Transactions on Medical Imaging, 2011, 30, 215-223.	8.9	103
273	Evaluation of Registration Methods on Thoracic CT: The EMPIRE10 Challenge. IEEE Transactions on Medical Imaging, 2011, 30, 1901-1920.	8.9	363
274	Automated Measurement of the Arteriolar-to-Venular Width Ratio in Digital Color Fundus Photographs. IEEE Transactions on Medical Imaging, 2011, 30, 1941-1950.	8.9	153
275	Modified Chrispin-Norman chest radiography score for cystic fibrosis: observer agreement and correlation with lung function. European Radiology, 2011, 21, 722-729.	4.5	13
276	Semi-automatic construction of reference standards for evaluation of image registration. Medical Image Analysis, 2011, 15, 71-84.	11.6	98
277	TIPS bilateral noise reduction in 4D CT perfusion scans produces high-quality cerebral blood flow maps. Physics in Medicine and Biology, 2011, 56, 3857-3872.	3.0	77
278	Association of the transfer coefficient of the lung for carbon monoxide with emphysema progression in male smokers. European Respiratory Journal, 2011, 38, 1012-1018.	6.7	22
279	Identification of Chronic Obstructive Pulmonary Disease in Lung Cancer Screening Computed Tomographic Scans. JAMA - Journal of the American Medical Association, 2011, 306, 1775-81.	7.4	123
280	CT-quantified emphysema in male heavy smokers: association with lung function decline. Thorax, 2011, 66, 782-787.	5.6	142
281	Automatic localization of bifurcations and vessel crossings in digital fundus photographs using location regression. Proceedings of SPIE, 2011, , .	0.8	1
282	Evaluation of a Computer-Aided Diagnosis System for Diabetic Retinopathy Screening on Public Data. , 2011, 52, 4866.		101
283	Computer-aided Diagnosis: How to Move from the Laboratory to the Clinic. Radiology, 2011, 261, 719-732.	7.3	230
284	Computer-Aided Detection of Ground Glass Nodules in Thoracic CT Images Using Shape, Intensity and Context Features. Lecture Notes in Computer Science, 2011, 14, 207-214.	1.3	15
285	Automated estimation of progression of interstitial lung disease in CT images. Medical Physics, 2010, 37, 63-73.	3.0	18
286	Automatic coronary calcium scoring in low-dose non-ECG-synchronized thoracic CT scans. Proceedings of SPIE, 2010, , .	0.8	1
287	Interactive annotation of textures in thoracic CT scans. Proceedings of SPIE, 2010, , .	0.8	5
288	Comparing and combining algorithms for computer-aided detection of pulmonary nodules in computed tomography scans: The ANODE09 study. Medical Image Analysis, 2010, 14, 707-722.	11.6	245

#	Article	IF	CITATIONS
289	Retinopathy Online Challenge: Automatic Detection of Microaneurysms in Digital Color Fundus Photographs. IEEE Transactions on Medical Imaging, 2010, 29, 185-195.	8.9	414
290	Automatic Segmentation of Pulmonary Lobes Robust Against Incomplete Fissures. IEEE Transactions on Medical Imaging, 2010, 29, 1286-1296.	8.9	83
291	Adaptive local multi-atlas segmentation: Application to the heart and the caudate nucleus. Medical Image Analysis, 2010, 14, 39-49.	11.6	139
292	Automatic determination of the artery vein ratio in retinal images. Proceedings of SPIE, 2010, , .	0.8	7
293	Interactive lung segmentation in CT scans with severe abnormalities. , 2010, , .		15
294	Automatic segmentation of intracranial arteries and veins in fourâ€dimensional cerebral CT perfusion scans. Medical Physics, 2010, 37, 2956-2966.	3.0	30
295	Automated aortic calcium scoring on lowâ€dose chest computed tomography. Medical Physics, 2010, 37, 714-723.	3.0	35
296	Rib suppression in chest radiographs to improve classification of textural abnormalities. , 2010, , .		9
297	Computer-aided Detection of Lung Cancer on Chest Radiographs: Effect on Observer Performance. Radiology, 2010, 257, 532-540.	7.3	66
298	Noise filtering in thin-slice 4D cerebral CT perfusion scans. , 2010, , .		4
299	Screening for Lung Cancer with Digital Chest Radiography: Sensitivity and Number of Secondary Work-up CT Examinations. Radiology, 2010, 255, 629-637.	7.3	41
300	Interactively learning a patient specific k-nearest neighbor classifier based on confidence weighted samples. , 2010, , .		1
301	Coronary Artery Calcification Scoring in Low-Dose Ungated CT Screening for Lung Cancer: Interscan Agreement. American Journal of Roentgenology, 2010, 194, 1244-1249.	2.2	51
302	Distribution of emphysema in heavy smokers: Impact on pulmonary function. Respiratory Medicine, 2010, 104, 76-82.	2.9	27
303	Reply to Hochheggar etÂal Respiratory Medicine, 2010, 104, 1074.	2.9	0
304	Comparing coronary artery calcium and thoracic aorta calcium for prediction of all-cause mortality and cardiovascular events on low-dose non-gated computed tomography in a high-risk population of heavy smokers. Atherosclerosis, 2010, 209, 455-462.	0.8	117
305	Computer-aided diagnosis in chest imaging: How to improve performance and avoid reinventing the wheel. , 2010, , .		1
306	Improving hard exudate detection in retinal images through a combination of local and contextual information. , 2010, , .		20

#	Article	IF	CITATIONS
307	Vessel tree extraction using locally optimal paths. , 2010, , .		16
308	Automatic segmentation of pulmonary vasculature in thoracic CT scans with local thresholding and airway wall removal. , 2010, , .		17
309	Active Learning for an Efficient Training Strategy of Computer-Aided Diagnosis Systems: Application to Diabetic Retinopathy Screening. Lecture Notes in Computer Science, 2010, 13, 603-610.	1.3	12
310	Fusion of Local and Global Detection Systems to Detect Tuberculosis in Chest Radiographs. Lecture Notes in Computer Science, 2010, 13, 650-657.	1.3	46
311	Simulation of Nodules and Diffuse Infiltrates in Chest Radiographs Using CT Templates. Lecture Notes in Computer Science, 2010, 13, 396-403.	1.3	2
312	Automatic lung segmentation from thoracic computed tomography scans using a hybrid approach with error detection. Medical Physics, 2009, 36, 2934-2947.	3.0	191
313	A linking framework for pixel classification based retinal vessel segmentation. Proceedings of SPIE, 2009, , .	0.8	7
314	Segmentation of arteries and veins on 4D CT perfusion scans for constructing arteriograms and venograms. , 2009, , .		1
315	Automatic detection of registration errors for quality assessment in medical image registration. Proceedings of SPIE, 2009, , .	0.8	6
316	Fast murine airway segmentation and reconstruction in micro-CT images. Proceedings of SPIE, 2009, , .	0.8	1
317	Airway segmentation and analysis for the study of mouse models of lung disease using micro-CT. Physics in Medicine and Biology, 2009, 54, 7009-7024.	3.0	34
318	Automatic classification of retinal vessels into arteries and veins. Proceedings of SPIE, 2009, , .	0.8	46
319	Registration of 3D spectral OCT volumes using 3D SIFT feature point matching. Proceedings of SPIE, 2009, , .	0.8	29
320	Active learning approach for detection of hard exudates, cotton wool spots, and drusen in retinal images. , 2009, , .		5
321	Automatic Segmentation of Pulmonary Segments From Volumetric Chest CT Scans. IEEE Transactions on Medical Imaging, 2009, 28, 621-630.	8.9	75
322	Multi-Atlas-Based Segmentation With Local Decision Fusion—Application to Cardiac and Aortic Segmentation in CT Scans. IEEE Transactions on Medical Imaging, 2009, 28, 1000-1010.	8.9	330
323	Information Fusion for Diabetic Retinopathy CAD in Digital Color Fundus Photographs. IEEE Transactions on Medical Imaging, 2009, 28, 775-785.	8.9	105
324	Comparison and Evaluation of Methods for Liver Segmentation From CT Datasets. IEEE Transactions on Medical Imaging, 2009, 28, 1251-1265.	8.9	848

#	Article	IF	CITATIONS
325	Noise Reduction in Computed Tomography Scans Using 3-D Anisotropic Hybrid Diffusion With Continuous Switch. IEEE Transactions on Medical Imaging, 2009, 28, 1585-1594.	8.9	81
326	Fast detection of the optic disc and fovea in color fundus photographs. Medical Image Analysis, 2009, 13, 859-870.	11.6	188
327	A large-scale evaluation of automatic pulmonary nodule detection in chest CT using local image features and k-nearest-neighbour classification. Medical Image Analysis, 2009, 13, 757-770.	11.6	270
328	Dissimilarity-based classification in the absence of local ground truth: Application to the diagnostic interpretation of chest radiographs. Pattern Recognition, 2009, 42, 1768-1776.	8.1	24
329	A comparison of six software packages for evaluation of solid lung nodules using semi-automated volumetry: What is the minimum increase in size to detect growth in repeated CT examinations. European Radiology, 2009, 19, 800-808.	4.5	144
330	Computer-aided diagnosis in chest radiography: Beyond nodules. European Journal of Radiology, 2009, 72, 226-230.	2.6	80
331	Computer-aided detection (CAD) of lung nodules and small tumours on chest radiographs. European Journal of Radiology, 2009, 72, 218-225.	2.6	32
332	Image Subtraction Facilitates Assessment of Volume and Density Change in Ground-Glass Opacities in Chest CT. Investigative Radiology, 2009, 44, 61-66.	6.2	16
333	Automatic Segmentation of the Pulmonary Lobes from Fissures, Airways, and Lung Borders: Evaluation of Robustness against Missing Data. Lecture Notes in Computer Science, 2009, 12, 263-271.	1.3	14
334	Evaluation of 4D-CT Lung Registration. Lecture Notes in Computer Science, 2009, 12, 747-754.	1.3	39
335	Global and Local Multi-valued Dissimilarity-Based Classification: Application to Computer-Aided Detection of Tuberculosis. Lecture Notes in Computer Science, 2009, 12, 724-731.	1.3	14
336	Computerâ€Aided Diagnosis in Thoracic Computed Tomography. Imaging Decisions (Berlin, Germany), 2008, 12, 11-22.	0.2	9
337	Supervised Enhancement Filters: Application to Fissure Detection in Chest CT Scans. IEEE Transactions on Medical Imaging, 2008, 27, 1-10.	8.9	65
338	Evaluation of a System for Automatic Detection of Diabetic Retinopathy From Color Fundus Photographs in a Large Population of Patients With Diabetes. Diabetes Care, 2008, 31, 193-198.	8.6	243
339	Automated detection of nodules attached to the pleural and mediastinal surface in low-dose CT scans. Proceedings of SPIE, 2008, , .	0.8	1
340	Evaluation of a System for Automatic Detection of Diabetic Retinopathy From Color Fundus Photographs in a Large Population of Patients With Diabetes. Diabetes Care, 2008, 31, e64-e64.	8.6	57
341	Vessel segmentation in 3D spectral OCT scans of the retina. , 2008, , .		46
342	Adaptive local multi-atlas segmentation: application to heart segmentation in chest CT scans. , 2008, , .		14

20

#	Article	IF	CITATIONS
343	Can the Extent of Low-Attenuation Areas on CT Scans Really Demonstrate Changes in the Severity of Emphysema?. Radiology, 2008, 247, 293-294.	7.3	7
344	Anniversary Paper: Image processing and manipulation through the pages of <i>Medical Physics</i> . Medical Physics, 2008, 35, 4488-4500.	3.0	8
345	Automated localization of the optic disc and the fovea. , 2008, 2008, 3538-41.		23
346	Integrating local voxel classification and global shape models for medical image segmentation. Proceedings of SPIE, 2008, , .	0.8	0
347	Robust Segmentation and Anatomical Labeling of the Airway Tree from Thoracic CT Scans. Lecture Notes in Computer Science, 2008, 11, 219-226.	1.3	43
348	Semi-automatic Reference Standard Construction for Quantitative Evaluation of Lung CT Registration. Lecture Notes in Computer Science, 2008, 11, 1006-1013.	1.3	38
349	Automated Detection and Differentiation of Drusen, Exudates, and Cotton-Wool Spots in Digital Color Fundus Photographs for Diabetic Retinopathy Diagnosis. , 2007, 48, 2260.		328
350	Automated detection of pulmonary nodules from low-dose computed tomography scans using a two-stage classification system based on local image features. , 2007, , .		13
351	Monitoring of Smoking-induced Emphysema with CT in a Lung Cancer Screening Setting: Detection of Real Increase in Extent of Emphysema. Radiology, 2007, 244, 890-897.	7.3	60
352	Detection of coronary calcifications from computed tomography scans for automated risk assessment of coronary artery disease. Medical Physics, 2007, 34, 1450-1461.	3.0	81
353	Computerâ€aided detection of interstitial abnormalities in chest radiographs using a reference standard based on computed tomography. Medical Physics, 2007, 34, 4798-4809.	3.0	29
354	Segmentation of the Optic Disc, Macula and Vascular Arch in Fundus Photographs. IEEE Transactions on Medical Imaging, 2007, 26, 116-127.	8.9	192
355	Automatic rib segmentation and labeling in computed tomography scans using a general framework for detection, recognition and segmentation of objects in volumetric data. Medical Image Analysis, 2007, 11, 35-46.	11.6	52
356	Local noise weighted filtering for emphysema scoring of low-dose CT images. IEEE Transactions on Medical Imaging, 2006, 25, 451-463.	8.9	71
357	Computer analysis of computed tomography scans of the lung: a survey. IEEE Transactions on Medical Imaging, 2006, 25, 385-405.	8.9	460
358	Automated classification of hyperlucency, fibrosis, ground glass, solid, and focal lesions in high-resolution CT of the lung. Medical Physics, 2006, 33, 2610-2620.	3.0	54
359	Bony Structure Suppression in Chest Radiographs. Lecture Notes in Computer Science, 2006, , 166-177.	1.3	11

A pattern recognition approach to enhancing structures in 3D CT data. , 2006, 6144, 569.

3

#	Article	IF	CITATIONS
361	Simulating nodules in chest radiographs with real nodules from multi-slice CT images. , 2006, , .		1
362	Improving computer-aided diagnosis of interstitial disease in chest radiographs by combining one-class and two-class classifiers. , 2006, 6144, 1684.		5
363	Segmentation of anatomical structures in chest radiographs using supervised methods: a comparative study on a public database. Medical Image Analysis, 2006, 10, 19-40.	11.6	433
364	Image structure clustering for image quality verification of color retina images in diabetic retinopathy screening. Medical Image Analysis, 2006, 10, 888-898.	11.6	128
365	A computer-aided diagnosis system for detection of lung nodules in chest radiographs with an evaluation on a public database. Medical Image Analysis, 2006, 10, 247-258.	11.6	134
366	Filter learning: Application to suppression of bony structures from chest radiographs. Medical Image Analysis, 2006, 10, 826-840.	11.6	50
367	Image Denoising with k-nearest Neighbor and Support Vector Regression. , 2006, , .		5
368	Image Classification from Generalized Image Distance Features: Application to Detection of Interstitial Disease in Chest Radiographs. , 2006, , .		2
369	Special Issue on Pulmonary Imaging. IEEE Transactions on Medical Imaging, 2006, 25, 381-384.	8.9	1
370	Segmentation of the posterior ribs in chest radiographs using iterated contextual pixel classification. IEEE Transactions on Medical Imaging, 2006, 25, 602-611.	8.9	76
371	Supervised Probabilistic Segmentation of Pulmonary Nodules in CT Scans. Lecture Notes in Computer Science, 2006, 9, 912-919.	1.3	15
372	Local noise reduction for emphysema scoring in low-dose CT images. , 2005, , .		0
373	Dimensionality reduction of image features using the canonical contextual correlation projection. Pattern Recognition, 2005, 38, 2409-2418.	8.1	14
374	Automated coronary calcification detection and scoring. Proc Int Symp Image Signal Process Anal, 2005, , .	0.0	2
375	Automatic detection of red lesions in digital color fundus photographs. IEEE Transactions on Medical Imaging, 2005, 24, 584-592.	8.9	422
376	Toward automated segmentation of the pathological lung in CT. IEEE Transactions on Medical Imaging, 2005, 24, 1025-1038.	8.9	205
377	Interactive segmentation of abdominal aortic aneurysms in CTA images. Medical Image Analysis, 2004, 8, 127-138.	11.6	105

A pattern recognition approach to automated coronary calcium scoring. , 2004, , .

#	Article	IF	CITATIONS
379	Static posterior probability fusion for signal detection: applications in the detection of interstitial diseases in chest radiographs. , 2004, , .		2
380	Pixel position regression - application to medical image segmentation. , 2004, , .		4
381	Automatic detection of calcifications in the aorta from CT scans of the abdomen1. Academic Radiology, 2004, 11, 247-257.	2.5	41
382	Comparative study of retinal vessel segmentation methods on a new publicly available database. , 2004, 5370, 648.		496
383	Ridge-Based Vessel Segmentation in Color Images of the Retina. IEEE Transactions on Medical Imaging, 2004, 23, 501-509.	8.9	2,914
384	Lung field segmentation from thin-slice CT scans in presence of severe pathology. , 2004, , .		16
385	Detection of interstitial lung disease in PA chest radiographs. , 2004, , .		2
386	Dimensionality Reduction by Canonical Contextual Correlation Projections. Lecture Notes in Computer Science, 2004, , 562-573.	1.3	9
387	Multi-scale texture classification from generalized locally orderless images. Pattern Recognition, 2003, 36, 899-911.	8.1	21
388	Multi-scale Nodule Detection in Chest Radiographs. Lecture Notes in Computer Science, 2003, , 602-609.	1.3	19
389	Automatic detection of calcifications in the aorta from abdominal CT scans. International Congress Series, 2003, 1256, 1037-1042.	0.2	3
390	Computer-aided diagnosis in high resolution CT of the lungs. Medical Physics, 2003, 30, 3081-3090.	3.0	122
391	Adapting Active Shape Models for 3D Segmentation of Tubular Structures in Medical Images. Lecture Notes in Computer Science, 2003, 18, 136-147.	1.3	97
392	Assessing the skeletal age from a hand radiograph: automating the Tanner-Whitehouse method. , 2003, , .		23
393	Segmenting the posterior ribs in chest radiographs by iterated contextual pixel classification. , 2003, ,		5
394	Interactive shape models. , 2003, 5032, 1206.		10
395	Model-based segmentation of abdominal aortic aneurysms in CTA images. , 2003, , .		10
396	Automated Segmentation of Abdominal Aortic Aneurysms in Multi-spectral MR Images. Lecture Notes in Computer Science, 2003, , 538-545.	1.3	6

#	Article	IF	CITATIONS
397	Active-shape-model-based segmentation of abdominal aortic aneurysms in CTA images. , 2002, , .		30
398	Automatic detection of abnormalities in chest radiographs using local texture analysis. IEEE Transactions on Medical Imaging, 2002, 21, 139-149.	8.9	193
399	Active shape model segmentation with optimal features. IEEE Transactions on Medical Imaging, 2002, 21, 924-933.	8.9	444
400	Detection of abnormal tissue in HRCT scans of the chest. , 2002, , 1101-1101.		0
401	Automatic segmentation and texture analysis of PA chest radiographs to detect abnormalities related to interstitial disease and tuberculosis. , 2002, , 685-688.		2
402	Computer-aided diagnosis in chest radiography: a survey. IEEE Transactions on Medical Imaging, 2001, 20, 1228-1241.	8.9	411
403	<title>Automatic delineation of ribs in frontal chest radiographs</title> . , 2000, 3979, 825.		11
404	Applications of Locally Orderless Images. Journal of Visual Communication and Image Representation, 2000, 11, 196-208.	2.8	11
405	Automatic segmentation of lung fields in chest radiographs. Medical Physics, 2000, 27, 2445-2455.	3.0	97
406	Texture histograms as a function of irradiation and viewing direction. International Journal of Computer Vision, 1999, 31, 169-184.	15.6	55
407	Reflectance and texture of real-world surfaces. ACM Transactions on Graphics, 1999, 18, 1-34.	7.2	1,065
408	Automatic Segmentation of Lung Fields in Chest Radiographs. Lecture Notes in Computer Science, 1999, , 184-191.	1.3	0
409	Diffuse and Specular Reflectance from Rough Surfaces. Applied Optics, 1998, 37, 130.	2.1	159
410	Surface bidirectional reflection distribution function and the texture of bricks and tiles. Applied Optics, 1997, 36, 3717.	2.1	8
411	<title>Surface BRDF and texture of bricks</title> . , 1996, , .		1
412	REALISE: reconstruction of REALity from Image SEquences. , 1996, , .		4
413	Reflectance and texture of real-world surfaces. , 0, , .		110

19

#	Article	IF	CITATIONS
415	Supervised segmentation by iterated contextual pixel classification. , 0, , .		10
416	Classifying convex sets for vessel detection in retinal images. , 0, , .		2
417	Improved Classification of Pulmonary Nodules by Automated Detection of Benign Subpleural Lymph Nodes. , 0, , .		5
418	Hybrid Diffusion Compared with Existing Diffusion Schemes on Simulated Low Dose CT Scans. , 0, , .		3